Cluster Lifetime Characterization for Vehicular Communication Channels

Mingming Gan[1], Zhinan Xu[1], Christoph F. Mecklenbräuker[2], Thomas Zemen[1,3]
[1] FTW Forschungszentrum Telekommunikation Wien, Vienna, Austria
[2] Institute of Telecommunications, Vienna University of Technology, Vienna, Austria
[3] AIT Austrian Institute of Technology, Vienna, Austria

***Abstract*—Simulating the time-variance of vehicular channels correctly remains a challenging topic. We are interested in parsimonious mathematical channel models, in which only significant groups of multipath components (MPCs) are included. The MPCs are grouped in the delay-Doppler domain, which enables the development of cluster-based channel models. However, the characterization of time-variant vehicular channel parameters based on a joint clustering-and-tracking framework has not been adequately studied previously.**

In this paper, we focus on the cluster lifetime characterization for vehicular communication channels. A joint cluster identification-and-tracking approach based on the local scattering function (LSF) is applied, which takes the delay and Doppler domains into consideration. The proposed approach uses a density-based spatial clustering of applications with noise (DBSCAN) algorithm for identification. The cluster centroid tracking is based on the multipath component distance (MCD) matrix. We apply this approach to real-world vehicular channel measurements. The time-varying cluster lifetimes are tracked according via the cluster centroids for two scenarios. The results indicate that the detected cluster related to the line-of-sight (LOS) component persists throughout the measurement run and contributes the highest gain level for both scenarios. The clusters detected from traffic signs and large moving vehicles also persist for a longer period, whereas many clusters associated with discrete scatterers along the roadside appear for very short periods.

I. Introduction

In recent years, vehicle-to-vehicle (V2V) communication systems have received a lot of interest. An understanding of V2V propagation channels is significant for the development of suitable communication standards. Vehicular communication channels are characterized by a non-stationary time- and frequency-selective fading process due to the fast changing propagation conditions. Local stationarity can be assumed for a finite region in time and frequency, so a time and frequency dependent local scattering function (LSF) is calculated [1]. Therefore, the wide-sense stationarity and uncorrelated-scattering (WSSUS) assumption holds approximately in this finite region [2]. The LSF is a multitaper estimate of the two-dimensional (2-D) power spectral density in delay and Doppler, where each peak is composed of several multipath components (MPCs) stemming from scatterers in the environment [3].

The well-known geometry-based stochastic channel modeling (GSCM) is an usual approach to model vehicular channels by placing scatterers randomly besides the link between transmitter (Tx) and receiver (Rx) according to a spatial distribution. However, from a Rx point of view, some contributions from MPCs in the received signal might be masked by the noise. In measured vehicular channels, it can be seen that the significant MPCs tend to be grouped in clusters based on the LSF [3], where the issue of cluster tracking over time is not addressed. We will use this observation to reduce the numerical complexity of GSCMs enabling a real time implementation for transceiver testing. Since clusters can be used to model time-variant scenarios, a reliable joint cluster identification-and-tracking approach is required [4].

In the present work, we present a joint cluster identification-and-tracking approach based on the power spectral density in delay and Doppler. *The contributions of this paper are fourfold:* i) We identify clusters for each stationarity region firstly based on the density-based spatial clustering for applications with noise (DBSCAN) algorithm. ii) The predicted cluster centroids are tracked according to the multipath component distance (MCD) matrix among the centroids. iii) We fully characterize the cluster lifetimes based on vehicular channel measurements data. iv) We analyze the cluster lifetimes corresponding to the geometry information of the measurements. Note that the cluster lifetime in this paper describes for how many stationarity regions a cluster exists. This parameter is significant for modeling the birth/death process of smoothly time-varying channels [5].

II. Identification-and-Tracking Approach

We calculate the LSF from measurement data firstly. Then we distinguish relevant MPCs based on the defined thresholds. Afterwards, the DBSCAN clustering algorithm is introduced for identification. Furthermore, we describe the idea for cluster tracking based on the distance between the clusters' centroids.

A. LSF Estimator

A significant feature of the vehicular channel is the fast-changing propagation conditions. Thus, the observed fading process is nonstationary. Due to the environment changes with a finite rate, the nonstationary can be overcome by

This work was performed in the FTW project Future ITS, a scientific cooperation co-funded by Kapsch TrafficCom AG, and Vienna University of Technology. The Austrian Competence Center FTW Forschungszentrum Telekommunikation Wien GmbH is funded within the program COMET - Competence Centers for Excellent Technologies by BMVIT, BMWFJ, and the City of Vienna. The COMET program is managed by the FFG.

approximating the fading process to be local stationarity for a region with finite extent in time and frequency [1]. The locally stationarity region is defined as having $M \times N$ samples in time and frequency, respectively. The total number of snapshots and frequency bins are denoted as S and Q, respectively. Therefore, the time index of each stationarity region is $k_t \in \{0, \cdots, \lfloor S/M-1 \rfloor\}$, and the frequency index of each stationarity region is $k_f \in \{0, \cdots, \lfloor Q/N-1 \rfloor\}$. k_t and k_f correspond to the center of each stationarity region. An estimate of the discrete LSF is defined as $\hat{C}[k_t, k_f; n, p]$ [2], where $n \in \{0, \cdots, N-1\}$ is the delay index, and $p \in \{-M/2, \cdots, M/2-1\}$ is the Doppler index. In our work, we are interested in $\hat{C}[k_t; n, p]$, where $k_f = 0$ because of $Q = N$. The LSF $\hat{C}[k_t; n, p]$ is a time-varying representation of the delay-Doppler spectrum.

B. Selection of Relevant MPCs

Among the received signal, there are several peaks with low gain compared to the highest peaks. These low peaks are not so important for the cluster identification. We use a simple concept as described in [3] to select the relevant peaks, where the peaks are related to the relevant MPCs. The concept is based on the threshold criterion, which defines that a path can exist only if its gain is higher than a certain threshold. This threshold is chosen as $-25\,\mathrm{dB}$ from the highest detected peak. In addition, we choose another threshold to remove the noise. It is defined that all components below the noise power plus $15\,\mathrm{dB}$ are set to 0. Both thresholds should be crosschecked to obtain the relevant MPCs for cluster identification. Each single MPC at stationarity region k_t is represented by a parameter vector $[\tau_l^{(k_t)}\ \nu_l^{(k_t)}\ P_l^{(k_t)}]^{\mathrm{T}}$ containing the delay, Doppler shift and its gain, where $l \in \{1, \ldots, L^{(k_t)}\}$ is the MPC index, $L^{(k_t)}$ is the total number of MPCs at k_t, and $[\cdot]^{\mathrm{T}}$ indicates the transpose.

C. DBSCAN Clustering Algorithm

The DBSCAN algorithm is a density-based clustering algorithm to discover clusters of arbitrary shape. The key concept of the DBSCAN algorithm is that for each point of a cluster, the neighborhood of a given radius Eps for each point p in one cluster has to contain at least a minimum number of points $MinPts$ [6]. The definition of DBSCAN is based on the notion of density-reachable. Firstly, a point p is directly density-reachable from a point q defined by fulfilling these two conditions: (i) p is not farther away than Eps, and (ii) q is surrounded by enough points, where the number of points should not be smaller than $MinPts$. The second condition is also called as core point condition. Based on this definition with respect to Eps and $MinPts$, a point p is density-reachable from a point q if there is a sequence of points $p_1, \cdots, p_n$ with $p_1 = p$ and $p_n = q$ in which each p_{i+1} is directly density-reachable from p_i. It is noteworthy that the density-reachable criteria is an asymmetric relation. Due to this asymmetry, another notion of the symmetric density-connected relation is defined with respect to Eps and $MinPts$. If there exists a point o such that both p and q are density-reachable from o, we call that p is density-connected to q. A cluster is a subset of the points of the database, which need to satisfy two conditions: (i) all points are density-connected in the cluster, and (ii) a point belongs to the cluster if it is density-reachable from any point of the cluster. In our work, the point is corresponding to the MPC. We set each cluster a cluster-ID (CLID) as c among all stationarity region k_t and the set of MPCs' indices in cluster c for stationarity region k_t as $\mathcal{I}_c^{(k_t)}$.

D. Cluster Tracking Approach

Cluster tracking is used to capture the movement of clusters. The idea for cluster tracking in our paper is based on the distance between the clusters' centroids for different stationarity regions. The cluster centroid $\boldsymbol{\mu}_c^{(k_t)}$ for stationarity region k_t is calculated as

$$\begin{aligned} \boldsymbol{\mu}_c^{(k_t)} &= [\tau_c^{(k_t)} \quad \nu_c^{(k_t)} \quad P_c^{(k_t)}]^{\mathrm{T}} \\ &= \begin{bmatrix} \frac{1}{\gamma_c^{(k_t)}} \sum_{l \in \mathcal{I}_c^{(k_t)}} P_l^{(k_t)} \tau_l^{(k_t)} \\ \frac{1}{\gamma_c^{(k_t)}} \sum_{l \in \mathcal{I}_c^{(k_t)}} P_l^{(k_t)} \nu_l^{(k_t)} \\ \frac{1}{L^{(k_t)}} \gamma_c^{(k_t)} \end{bmatrix}, \end{aligned} \tag{1}$$

where $\gamma_c^{(k_t)} = \sum_{l \in \mathcal{I}_c^{(k_t)}} P_l^{(k_t)}$ is the cluster gain.

The subsequent sets of old $C^{(k_t)}$ and new $C^{(k_t+1)}$ cluster centroids $\boldsymbol{\mu}_{c_{\text{old}}}^{(k_t)}$ and $\boldsymbol{\mu}_{c_{\text{new}}}^{(k_t+1)}$, are considered, where $k_t + 1 \leq \lfloor S/M-1 \rfloor$, $c_{\text{old}} \in \{1, \cdots, C^{(k_t)}\}$ and $c_{\text{new}} \in \{1, \cdots, C^{(k_t+1)}\}$ are the cluster centroids' indices at k_t and $k_t + 1$, respectively. The MCD is chosen as suitable distance matrix between the centroids $\boldsymbol{\mu}_{c_{\text{old}}}^{(k_t)}$ and $\boldsymbol{\mu}_{c_{\text{new}}}^{(k_t+1)}$, with elements defined as [5]

$$\begin{aligned} [\boldsymbol{D}]_{c_{\text{old}} c_{\text{new}}} &= \mathrm{MCD}(\boldsymbol{\mu}_{c_{\text{old}}}^{(k_t)}, \boldsymbol{\mu}_{c_{\text{new}}}^{(k_t+1)}) \\ &= \sqrt{[\boldsymbol{D}]^2_{\tau, c_{\text{old}} c_{\text{new}}} + [\boldsymbol{D}]^2_{\nu, c_{\text{old}} c_{\text{new}}} + [\boldsymbol{D}]^2_{P, c_{\text{old}} c_{\text{new}}}}, \end{aligned} \tag{2}$$

where $[\boldsymbol{D}]^2_{\tau, c_{\text{old}} c_{\text{new}}}$, $[\boldsymbol{D}]^2_{\nu, c_{\text{old}} c_{\text{new}}}$ and $[\boldsymbol{D}]^2_{P, c_{\text{old}} c_{\text{new}}}$ are the squared Euclidean distance for the delay, Doppler and gain domain, respectively [7]. The dimension of the distance matrix $\boldsymbol{D}$ is $C^{(k_t)} \times C^{(k_t+1)}$. It can be seen that the MCD allows to combine the parameters that come in different units. All further steps of the cluster tracking algorithm can be easily done by searching in $\boldsymbol{D}$. Based on this distance matrix, it can be seen that the tracked cluster centroid for the new stationarity region $k_t + 1$ is only related to the cluster centroid at the stationarity region k_t. To track a cluster, the searching procedure in $\boldsymbol{D}$ works as [8]

- For each new centroid, the smallest value in each column of $\boldsymbol{D}$ is searched. The indices $c_{\text{old}}{}^* c_{\text{new}}{}^*$ of this value identifies the closest old cluster. If $[\boldsymbol{D}]_{c_{\text{old}}{}^* c_{\text{new}}{}^*}$ is larger than a specified threshold ε, the cluster related to this new centroid would be treated as a new cluster with a new CLID.
- For each old centroid, the number of close new centroids smaller than ε in each row of $\boldsymbol{D}$ is counted. If the number is one, the cluster related to this old centroid is seen moving. If the number is more than one, the cluster related to this old centroid is treated as a moving cluster

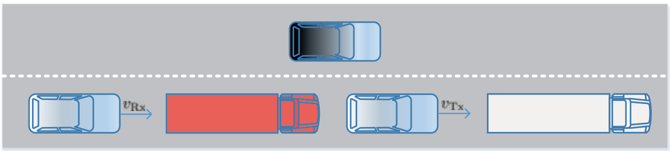

(a) LOS Obstruction Scenario

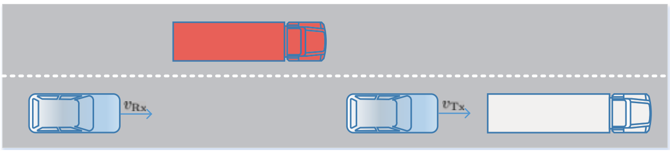

(b) LOS Scenario

Fig. 1. 2-D top view of the measurements scenarios.

towards the closest new one. In addition, we check each cluster among the other close ones whether it has been already counted as a new cluster. If yes, this cluster would use the same CLID as the found one. If not, the cluster is treated as a new cluster with a new CLID.

We can observe that the unique CLID is assigned to a new cluster, while the moved cluster inherits the CLID from its predecessor. Based on this, we could analyze the cluster lifetime, which means how many stationarity regions the cluster exists. Note that clusters never re-appear after they vanished based on the cluster algorithm. It further means that the cluster lifetime ends when it vanishes.

III. Measurement Data

The measurements used in the present work were collected in the DRIVEWAY'09 measurement campaign [9] conducted in Lund, Sweden. The channel impulse response is measured with a time resolution of $t_{\mathrm{s}} = 307.2\,\mu$s. The total time interval is $T = 10\,$s. Therefore, there are $S = 32000$ snapshots in total. The carrier frequency is $f_{\mathrm{c}} = 5.6\,$GHz within a bandwidth of $B = 240\,$MHz. Both Tx and Rx car are mounted with a linear array with four circular patch antennas perpendicular to the driving direction. The antennas cover the four main propagation directions due to their main lobes [10]. In order to achieve a $360°$ coverage in the azimuth plane, we consider to combine the antenna radiation pattern in this paper. We select two scenarios to analyze: (i) A truck obstructing line-of-sight (LOS) scenario, where the Tx and Rx drive in the same direction on a highway at around $75\,$km/h. The Tx drives in front. There is one truck in between Tx and Rx on the same lane and a car drives by on the left lane. In addition, there is a truck in the front of the Tx. A 2-D top view of this scenario is shown in Fig. 1(a). (ii) A LOS scenario shown in Fig. 1(b), where the Tx and Rx also drive in the same direction on a highway at around $90\,$km/h. One truck is driving on the left lane, while the other truck is in front of Tx. For both scenarios, there are some traffic signs along the highway. Meanwhile, some vehicles drive in the opposite direction on the other lane of the highway.

IV. Simulation Results

We calculate the LSF from measurement data firstly, where $S = 32000$ snapshots are divided in stationarity regions

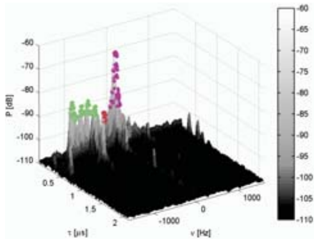

(a) $k_t = 1$

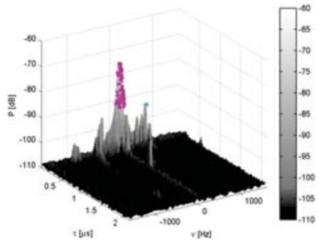

(b) $k_t = 245$

Fig. 2. An example of 2-D view of LSF and cluster identification at $k_t = 1$ and $k_t = 245$.

of $M = 128$ samples length. The stationarity regions are indexed by $k_t \in \{0, \ldots, 249\}$ for our case. The relevant MPCs are detected and the identification-and-tracking approach is applied. We choose the parameters as $Eps = 10$, $MinPts = 1$ and $\varepsilon = 5$. An exemplary plot based on the measurements for the LOS obstruction scenario is shown in Fig. 2. Different clusters are sketched with different colors, where the detected peaks in the same cluster are marked with the same color. The LSFs are corresponding to $k_t = 1$ and $k_t = 245$, from which it can be observed that a new cluster is appearing at $k_t = 245$, while two old clusters are vanishing comparing with $k_t = 1$.

A. Analysis for LOS Obstruction Scenario

For the LOS obstruction scenario, there are 132 clusters detected over the total time interval. Fig. 3(a) plots the detected number of clusters per stationarity region. More clusters are detected during the second half of the measurement: 5 clusters are more often detected during the first half of the measurement, while 2 clusters are usually detected during the second half of the measurement. The tracked cluster lifetimes are shown in Fig. 3(b), where $t^{(k_t)}$ denotes the time corresponding to the stationarity region index k_t, and the length of the horizontal lines indicate the lifetime of the relevant CLID. It can be observed that many clusters only exit for one stationarity region, which can not be tracked. We mark the clusters who exist more than 15 stationarity regions, equivalent to $0.59\,$s, in Fig. 3(b). In total, there are 7 marked clusters. Without considering the longest and shortest lifetimes, the distribution of the probability density of cluster lifetimes obeys a lognormal distribution with its parameters $\mu = 1.46$ and $\sigma = 0.72$, shown in Fig. 3(c).

A 2-D view of the cluster centroids tracking for the LOS obstruction scenario is shown in Fig. 4, where we select the clusters who exist more than 15 stationarity regions, equivalent to $0.59\,$s. A close-up 3-D view of the relevant CLIDs is also included in Fig. 4. According to the geometrical information of measurements, we divide the clusters into three categories: (i) It can be analyzed that the detected cluster $c = 1$, which remains throughout the entire measurement run and contributes the highest gain level. Its Doppler shift is around $0\,$Hz. (ii) For the clusters $c \in \{5, 13, 53, 108\}$, the delay and Doppler shift values for each cluster change slowly during their cluster lifetimes, respectively. In addition, due to the negative Doppler shifts, we evaluate that the most feasible case is that these clusters come from the traffic signs and the big vehicles.

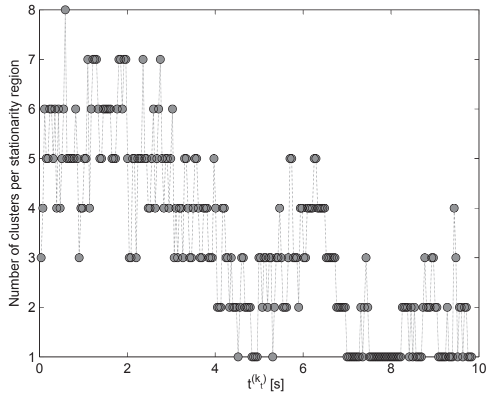

(a) Number of clusters

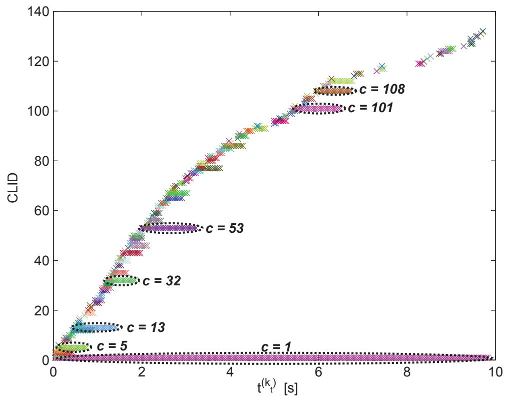

(b) Cluster lifetimes

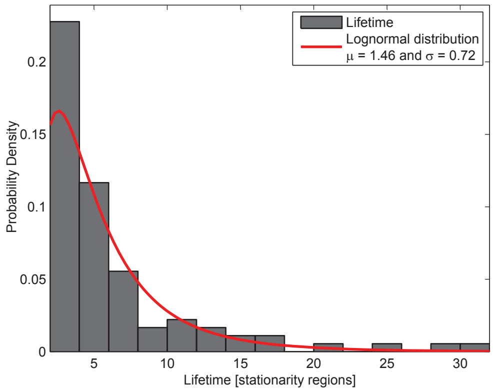

(c) Distribution

Fig. 3. Number of clusters per stationarity region, cluster lifetimes and its lognormal distribution for the LOS obstruction scenario.

These big vehicles drive faster than the Rx vehicle in the same direction, or drive slower than the Rx vehicle in the opposite direction. (iii) For the clusters $c \in \{32, 101\}$, it can be seen that their Doppler shifts are almost constant, while their delay values are changing considerably during their cluster lifetimes. We consider they are from moving big vehicles in the opposite direction on the other lane of the highway.

B. Analysis for LOS Scenario

For the LOS scenario, there are 47 clusters detected over the total time interval. During the whole measurement, 3 clusters are more often detected, shown in Fig. 5(a). Compared with

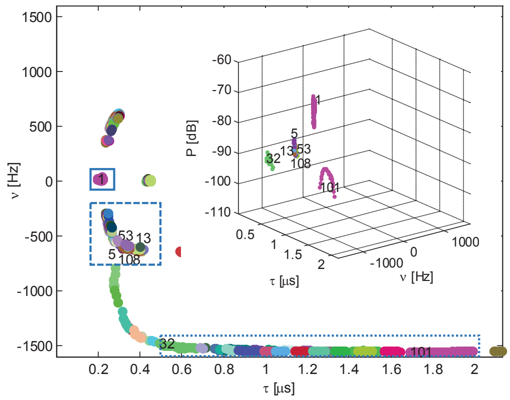

Fig. 4. Cluster centroids tracking for the LOS obstruction scenario, where the clusters who exist more than 15 stationarity regions are marked. A 3-D view of the relevant clusters is also included.

the LOS obstruction scenario, there are 6 clusters that remain for more than 15 stationarity regions in Fig. 5(b). Without considering the longest and shortest lifetimes, the distribution of the probability density of cluster lifetimes, shown in Fig. 5(c), also obeys a lognormal distribution with its parameters $\mu = 2.04$ and $\sigma = 1.05$.

The cluster centroids tracking for the LOS scenario is shown in Fig. 6. As for the LOS obstruction scenario, we select the clusters who exist more than 15 stationarity regions as well. Moreover, we can also observe three categories of clusters: (i) The cluster $c = 1$ is corresponding to the LOS component. Comparing the close-up 3-D view of the relevant CLIDs in Fig. 4 and Fig. 6, it can be seen that the contributed gain level by cluster $c = 1$ in the LOS scenario is higher than the one in the LOS obstruction scenario. (ii) For the clusters $c \in \{2, 3, 9, 12, 13, 24, 32, 39, 42, 44, 46\}$, their Doppler shifts are around $0\,\mathrm{Hz}$, which means that the clusters have the same speed as the Rx vehicle or the direction of the propagation path is orthogonal to the driving direction of the Rx vehicle. Meanwhile, their delays are approximately constant during their existing time, respectively. It indicates that the propagation path length stays the same for each cluster. Thus, we think these clusters come from the truck driving on the left lane, the big moving vehicles on the left lane, a bridge under which the Rx crosses at around $t^{k_t} = 1.5\,\mathrm{s}$, and the road signs where the Rx passing by is about $t^{k_t} = 8\,\mathrm{s}$. (iii) For the cluster $c = 27$, its delays are approximately constant, while its Doppler shifts become larger during its lifetime. It mostly comes from a big moving vehicle driving on the left lane, whose speed is increasing.

V. Conclusion

In this paper, we presented a joint cluster identification-and-tracking approach based on the LSF. We separated only the relevant MPCs from the Rx point of view based on the defined thresholds. Then the DBSCAN algorithm was used for the cluster identification. Furthermore, a low-complexity tracking algorithm relying on the MCD matrix was applied to track the cluster centroids. According to this approach, we

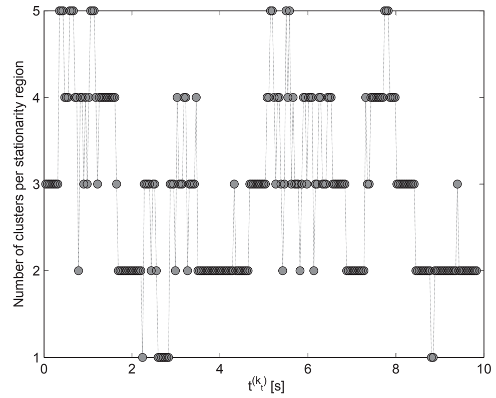

(a) Number of clusters

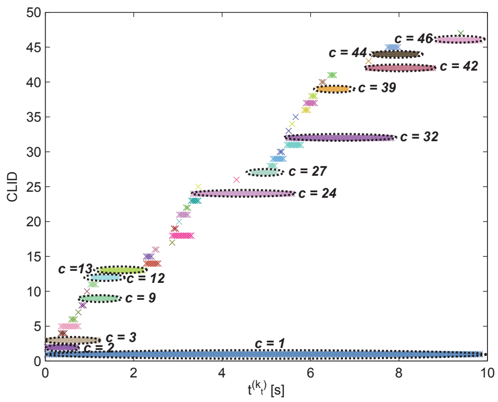

(b) Cluster lifetimes

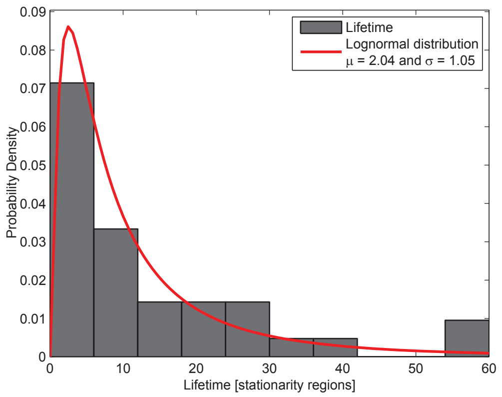

(c) Distribution

Fig. 5. Number of clusters per stationarity region, cluster lifetimes and its lognormal distribution for the LOS scenario.

evaluated the time-varying cluster lifetimes for two scenarios of vehicular channel measurements: (i) LOS obstruction scenario and (ii) LOS scenario. For both scenarios, without considering the longest and shortest lifetimes, the distribution of the probability density of cluster lifetimes obeys the log-normal distribution. In addition, combining the geometrical information of measurements, we analyzed where the clusters come from. For both scenarios, the clusters can be divided into three categories according to the properties of the delays and Doppler shifts. It can be seen that besides the cluster related to the LOS component, the clusters detected from the traffic signs and moving big vehicles also remain for a long time period,

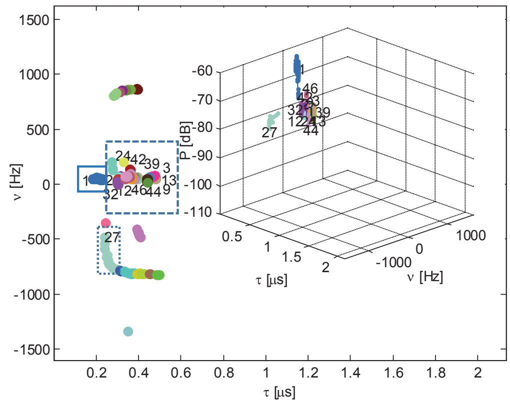

Fig. 6. Cluster centroids tracking for the LOS obstruction scenario, where the clusters who exist more than 15 stationarity regions are marked. A 3-D view of the relevant clusters is also included.

while lots of clusters coming from discrete scatterers along the road exist only for a very short time. The cluster lifetime characterization for vehicular communication channels will help researcher to develop a simple and accurate vehicular channel model.

References

[1] G. Matz, "Doubly underspread non-WSSUS channels: analysis and estimation of channel statistics," in *Signal Processing Advances in Wireless Communications, 2003. SPAWC 2003. 4th IEEE Workshop on*, June 2003, pp. 190–194.

[2] L. Bernadó, T. Zemen, F. Tufvesson, A. Molisch, and C. Mecklenbräuker, "Delay and Doppler spreads of nonstationary vehicular channels for safety-relevant scenarios," in *Vehicular Technology, IEEE Transactions on*, vol. 63, no. 1, Jan 2014, pp. 82–93.

[3] L. Bernadó, A. Roma, A. Paier, T. Zemen, N. Czink, J. Karedal, A. Thiel, F. Tufvesson, A. Molisch, and C. Mecklenbräuker, "In-tunnel vehicular radio channel characterization," in *Vehicular Technology Conference (VTC Spring), 2011 IEEE 73rd*, May 2011, pp. 1–5.

[4] N. Czink, R. Tian, S. Wyne, F. Tufvesson, J.-P. Nuutinen, J. Ylitalo, E. Bonek, and A. Molisch, "Tracking time-variant cluster parameters in MIMO channel measurements," in *Communications and Networking in China, 2007. CHINACOM '07. Second International Conference on*, Aug. 2007, pp. 1147–1151.

[5] N. Czink, "The random-cluster model - a stochastic MIMO channel model for broadband wireless communication systems of the 3rd generation and beyond," in *PHD Thesis*, 2007.

[6] M. Ester, H. peter Kriegel, J. S, and X. Xu, "A density-based algorithm for discovering clusters in large spatial databases with noise," in *2nd ACM International Conference on Knowledge Discovery and Data Mining (KDD)*. AAAI Press, Aug. 1996, pp. 226–231.

[7] N. Czink, P. Cera, J. Salo, E. Bonek, J. Nuutinen, and J. Ylitalo, "Automatic clustering of MIMO channel parameters using the multi-path component distance measure," in *Proceedings of WPMC 2005*, Aalborg, Dänemark, Sep. 2005.

[8] N. Czink, C. Mecklenbräuker, and G. Del Galdo, "A novel automatic cluster tracking algorithm," in *Personal, Indoor and Mobile Radio Communications, 2006 IEEE 17th International Symposium on*, Sep. 2006, pp. 1–5.

[9] A. Paier, L. Bernadó, J. Karedal, O. Klemp, and A. Kwoczek, "Overview of vehicle-to-vehicle radio channel measurements for collision avoidance applications," in *Vehicular Technology Conference (VTC 2010-Spring), 2010 IEEE 71st*, May 2010, pp. 1–5.

[10] A. Thiel, O. Klemp, A. Paier, L. Bernado, J. Karedal, and A. Kwoczek, "In-situ vehicular antenna integration and design aspects for vehicle-to-vehicle communications," in *Antennas and Propagation (EuCAP), 2010 Proceedings of the Fourth European Conference on*, April 2010, pp. 1–5.